

Cytonuclear diversity underlying clock and growth adaptation to warming environments in wild barley (*Hordeum vulgare* ssp. *spontaneum*)

Eyal Fridman¹, Lalit Tiwari¹, Eyal Bdolach¹, Manas Prusty¹, Avital Beery¹, Schewach Bodenheimer¹, Adi Doron-Faigenboim¹, Eiji Yamamoto², and Khalil Kashkush³

¹Agricultural Research Organization Volcani Center

²Meiji Daigaku Nogakubu Daigakuin Nogaku Kenkyuka

³Ben-Gurion University of the Negev Department of Life Sciences

December 1, 2022

Abstract

In plants, neither the contribution of the plasmotype in controlling circadian clock plasticity and overall plant robustness, nor what may be the fitness consequences of clock plasticity on genetic make-up has been fully elucidated. Here, we investigated the cytonuclear genetics underlying thermal plasticity of clock rhythmicity and fitness traits in reciprocal doubled haploid population and a diversity panel of wild barley (*Hordeum vulgare* ssp. *spontaneum*). We identified a positive correlation between the thermal plasticity of clock and vegetative growth with the robustness of reproductive output. Moreover, we identified significant linkage disequilibrium and epistatic interactions between previously identified drivers of clock (DOC) loci and the chloroplastic *RpoC1* genes, indicating adaptive value for specific cytonuclear gene combinations. Finally, heterologous over-expression of two barley *RpoC1* alleles in *Arabidopsis* showed significantly differential plasticity under elevated temperatures. Our results unravel previously unknown cytonuclear interactions as well as specific alleles within the chloroplastic genome that control clock thermal plasticity while also having pleiotropic effects on plant fitness in the field. The evolutionary and functional relationship between nuclear and chloroplastic DOCs suggest that adaptation to warming environments involve cytonuclear changes to confer local adaptation.

Cytonuclear diversity underlying clock and growth adaptation to warming environments in wild barley (*Hordeum vulgare* ssp. *spontaneum*)

Corresponding author:

Eyal Fridman

Plant Sciences Institute, Volcani Agricultural Research Organization (ARO), Bet Dagan, Israel

Tel: +972 3 968 3901

Fax: +972 3 966 9583

Running title: Cytonuclear control of clock and fitness robustness in wild barley

Lalit Dev Tiwari*¹, Eyal Bdolach*^{1,2}, Manas Ranjan Prusty¹, Avital Beery¹, Schewach Bodenheimer^{1, 3}, Adi Faigenboim-Doron¹, Eiji Yamamoto⁴, Khalil Kashkush², Eyal Fridman¹

¹Plant Sciences Institute, Volcani Agricultural Research Organization (ARO), Bet Dagan, Israel

² Department of Life Sciences, Ben-Gurion University, 84105, Beer-Sheva, Israel

³The Robert H. Smith Institute of Plant Sciences and Genetics in Agriculture, The Hebrew University of Jerusalem, Rehovot 76100, Israel

⁴ Graduate School of Agriculture, Meiji University 1-1-1 Higashi-Mita, Tama-ku, Kawasaki, Kanagawa, 214-8571, Japan

This work was supported by grants from the Israel Science Foundation (ISF 444/21) and Horizon2020/CAPITALISE AMD-862201-2 grants to E.F.

*These authors contributed equally to this work

Corresponding author email: fridmane@agri.gov.il

Abstract

In plants, neither the contribution of the plasmotype in controlling circadian clock plasticity and overall plant robustness, nor what may be the fitness consequences of clock plasticity on genetic make-up has been fully elucidated. Here, we investigated the cytonuclear genetics underlying thermal plasticity of clock rhythmicity and fitness traits in reciprocal doubled haploid population and a diversity panel of wild barley (*Hordeum vulgare* ssp. *spontaneum*). We identified a positive correlation between the thermal plasticity of clock and vegetative growth with the robustness of reproductive output. Moreover, we identified significant linkage disequilibrium and epistatic interactions between previously identified drivers of clock (DOC) loci and the chloroplastic *RpoC1* genes, indicating adaptive value for specific cytonuclear gene combinations. Finally, heterologous over-expression of two barley *RpoC1* alleles in *Arabidopsis* showed significantly differential plasticity under elevated temperatures. Our results unravel previously unknown cytonuclear interactions as well as specific alleles within the chloroplastic genome that control clock thermal plasticity while also having pleiotropic effects on plant fitness in the field. The evolutionary and functional relationship between nuclear and chloroplastic DOCs suggest that adaptation to warming environments involve cytonuclear changes to confer local adaptation.

Introduction

Plants are composed of cells in which three different organelle genomes co-evolved to cope with a dynamic environment: the nuclear genome (nucleotype), and the chloroplast and mitochondrial genomes (plasmotype). Environmental constraints promote the selection of causal mutations in all of those genomes. At the same time, epistatic relationships between nucleotypic and plasmotypic loci, and co-evolution of adaptive gene complexes are able to promote adaptation to dynamic environment and further to shape genetic make-up owing to preference of specific gene complexes (Groen *et al.*, 2022). In recent years, several studies have shown that phenotypic effects are related to the genetic diversity of the plasmotype and its interactions with the nucleotype (Joseph *et al.*, 2013; Tang *et al.*, 2014; Roux *et al.*, 2016). An elegant use of the haploid-inducer line available in *Arabidopsis* (*GFP-tailswap*) (Ravi *et al.*, 2014), allowed the generation of a set of reciprocal and isogenic cybrids from several accessions that were phenotyped for metabolism and photosynthesis under different light conditions (Flood *et al.*, 2020). Genetic analysis revealed that the nucleotype, plasmotype and their interaction accounted for 91.9%, 2.9% and 5.2% of genetic variation, respectively, thus highlighting the importance of interactions between nucleotype and plasmotype.

In crop plants and their wild relatives, few reports exist on the contribution of cytonuclear interactions (CNI) to a plant's phenotype and even less on its effects on its phenotypic plasticity. Examples, where the contribution of plasmotype to yield and grain quality has been demonstrated, exist in grasses (Frei *et al.* 2003; Sanetomo & Gebhardt, 2015). In cucumber, (Gordon & Staub, 2011) used reciprocal backcrosses between chilling-sensitive and chilling-tolerant lines to show that tolerance to reduced temperature is maternally inherited. Likely, these traits are the result of a local adaptation of the original wild alleles, since for example in bread wheat (*Triticum aestivum*), cytoplasmic influence on fruit quality is affected by genotype-by-environment interactions (Ekiz *et al.*, 1998). Nevertheless, many of these examinations of alloplasmic lines, which contained cytoplasm from distantly related wild relatives showed that effects on agronomic traits (rather than protein quality) are not frequent (Frei *et al.*, 2010). In maize, although cytoplasmic effects were

not significant between the direct and reciprocal populations, the interactions among the plasmotype and the nucleotype quantitative trait loci (QTL) were detected for both days to tassel and days to pollen shed (Tang *et al.*, 2014), further enforcing the increased explained variation between *Arabidopsis* cybrids when CNI are included (Flood *et al.*, 2020).

Circadian clock rhythms in plants are intertwined with chloroplastic activities including photosynthetic parameters such as NPQ and Φ PSII, whose values correlate with plant productivity (Kromdijk *et al.*, 2016). This insight led to the development of several high-throughput methods that measure the rhythmicity of the leaf chlorophyll fluorescence as an approximation to the period, phase and amplitude of the core clock (Gould *et al.*, 2009; Tindall *et al.*, 2015; Dakhiya *et al.*, 2017). The ability to measure hundreds of plants allowed for a comparison between species (Rees *et al.*, 2019), and to quantify the impact of temperature and soil composition on period and amplitude (Dakhiya *et al.*, 2017). Using the SensyPAM platform, which allows to infer photosynthetic rhythms based on repeated measurements of chlorophyll fluorescence (Bdolach *et al.*, 2019), we recently analyzed wild, landrace, and cultivar panels of barley as well as interspecific populations. We showed that some of the nuclear loci that control the photosynthetic rhythms were under selection during domestication. This could explain how modern crops lost the thermal plasticity of photosynthetic rhythms while maintaining a robust core clock (Prusty *et al.*, 2021). Furthermore, pleiotropic effects of these *drivers of clocks (DOCs)* loci on grain yield under stress indicate the adaptive value of clock plasticity. Nevertheless, this study did not consider the possible role of plasmotype diversity in modulating the effect of *DOCs* loci on circadian clock and fitness outputs, nor it examined the possibility that these effects on the clock plasticity may have been under selection also within the wild. Notably, previous studies identified the correlation of molecular evolution (i.e. dN/dS ratio) between genes encoding the plastid-encoded RNA polymerase (PEP) protein complex and nuclear genes (sig1-6) (Zhang *et al.*, 2015), which are ruled by the core clock genes (Belbin *et al.*, 2017). However, whether such selective forces acted on loci that regulate the output rather than the core rhythm of the clock remains unknown.

Here, we followed up on the photosynthetic rhythm analysis of a reciprocal bi-parental doubled haploid (DH) population segregating for both nucleotype and plasmotype (either “Ashkelon” or “Mount Hermon”) (Bdolach *et al.*, 2019). Photosynthetic rhythms measurements previously showed a significant difference of 2.2 h in the period between the carriers of the different plasmotypes (Bdolach *et al.*, 2019). Whole chloroplast genome sequencing of the two chloroplast identified several non-synonymous candidate polymorphism that could underlie these changes, including a N571K in the *rpoC1*. In the current study, we wished to, 1) extend the analysis of the plasmotype effects by including fitness traits and test if there is pleiotropy for QTL identified for clock output rhythmicity and life history traits, and 2) extend the breadth of diversity tested by examining the larger Barley1K collection with a new SNP genotyping array and identify possible DOC loci and, 3) to look into cytonuclear interactions (CNI) and their possible consequences on genetic make-up by analyzing B1K collection and a derived reciprocal F2 population, and finally, 4) test the functional consequence of variation in the *RpoC1* gene (Bdolach *et al.*, 2019) on photosynthetic rhythm plasticity by heterologous expression of two barley alleles in model plant *Arabidopsis*.

MATERIALS AND METHODS

2.1 Plant material

The source for the ASHER and reciprocal hybrids lines (RHL) populations described in this study are barley accessions (*Hordeum vulgare*ssp. *spontaneum*) that we selected from the Barley1K collection in Israel to represent the different genetic clades (Hubner *et al.*, 2009). In addition, the HID386 is from the IPK collection (Maurer *et al.*, 2015). The wild accessions are from Yerucham (B1K-02-02), Michmoret (B1K-03-09), Ein Prat (B1K-04-04), Neomi (B1K-05-07), Ashqelon (B1K-09-07), Mount Arbel (B1K-29-13), Mount Harif (B1K-33-09), Jordan Canal (B1K-42-16), Mount Eitan (B1K-49-19), Mount Hermon (B1K-50-04) and Kisalon, Israel (HID386). The ASHER is an F3 DH population generated from two reciprocal hybrids between Ashkelon (B1K-09-07) and Mount Hermon (B1K-50-04) and we described it in detail earlier (Bdolach *et al.*, 2019). The RHL that differ in their plasmotypes were obtained by two-way intercrossing between 11 wild accessions (from the B1K and HID386) and Noga.

2.2 Growth and phenotyping.

We conducted the net house experiments in the Agricultural Research Organization - Volcani (ARO) Center, Israel following similar sowing and transplanting as described previously for water limitation experiments by (Merchuk-Ovnat *et al.*, 2018) . Due to the sensitivity of wild barley to day-length conditions, we preferred to achieve mild higher temperature conditions by warming the nethouse rather than late sowing conducted for example for tomato (Bineau *et al.*, 2021). The thermal differences between HT and AT is depicted in Figure **S1** , with a mean increase of 3.9 °C and 2.8 °C during day and night time and maximum delta of mean 7.5 °C between AT to HT.

We obtained the life history traits phenotype for the ASHER population lines during winter of 2017-2018 in six replicates per treatment. The reciprocal hybrids lines population were grown during winter of 2019-2020. We began phenotyping by measuring Tiller height (TH), that is the length of the longest tiller from ground level to the last fully expended leaf in th at tiller. Tiller number (TN) is the number of tillers per plant and it was determined about one month after transplanting the plants. TH and TN were measured once (.1) or twice (.2) with 14 days apart. We calculated TH rate by suspending TH_2 with TH_1 and dividing with the number of days between these two measurements. We determined the number of days to flowering (DTF) based on the date when the first awns appear in the main tiller. During grain filling we measured five spikes per plant for spike length (SL) and later to obtain SLCV. In addition, during grain filling we measured plant height (PH) from ground to the start of the toolset spike. We then cached the five and whole spikes of each plant in separate paper and nylon bags, respectively. Plants were left to dry for several weeks after irrigation was terminated. We harvested dry plants by cutting at soil level and placing them in the nylon bags. Weight of the nylon bag with the plant is the total dry matter (TDM). We collected dispersal units from bag and weighted them. We calculated average spike dry weight (ASDW) based on weighing the five spikes that we cached in the paper bag. We then summed the weight of spikes (dispersal units) in the plastic and paper bags to obtain spikes dry weight (SpDW). Vegetative dry weight (VDW) is the reduction of SpDW from TDM.

We measured circadian clock amplitude and period in high-throughput SensyPAM (SensyTIV, Aviel, Israel) custom-designed to allow Fluorescence measurements under optimal temperature of 22°C (OT) or high temperature of 32°C (HT) as previously described (Bdolach *et al.* , 2019).

2.3 Allele mining and design of a genotyping platform for wild barley (*Hordeum vulgare* ssp. *spontaneum*)

We collected all the available DNA sequencing data, including SSR (Hubner *et al.* , 2009), BOPA1 (Schmalenbach *et al.*, 2011), Exome-Seq (Looseley *et al.*, 2017), and Genotype-by-sequencing (Chang *et al.* , 2022). The workflow for designing and eventually selecting informative SNP for the GWAS analysis is depicted in Figure**S2** . This harvest identified 502K unique contigs. After filtering these SNPs with MAF>0.05, no heterozygosity, a total read coverage >20, and missing marker>0.2 in at least 80% of the samples, we were left with 38K markers. We then retrieved 100 bp sequence flanking each marker and carried out BLAST search against the reference genome MorexV1 IBSCV2 barley genome to assure their identity and selectively singleton unique markers. Finally, we filtered out the redundant markers and reached approximately 30K markers sent to LGC Genomics Ltd. (GmbH, Germany) to design the probe set. During the probe design, the low specificity probes and probes with an off-target hit were removed, and it ended with 22.7K SNPs on the SNP chip made by LGC (Queens Road, Teddington, Middlesex, TW11 0LY, UK).

2.4 Statistical analysis

The JMP version 14.0 statistical package (SAS Institute, Cary, NC, USA) was used for statistical analyses. Student's t-Tests between treatments, plasmotypes and alleles were conducted using the 'Fit Y by X' function. A factorial model was employed for the analysis of variance (ANOVA), using 'Fit model', with temperature or plasmotype treatment and allelic state as fixed effects.

2.5 B1K accessions chloroplast DNA sequencing

From previous DNA shot-gun sequencing we realized that chloroplast isolation and sequencing were necessary

to overcome possible confounding effects of the known transfers that occur from plastid to nuclear [nuclear plastid DNAs (NUPTs)] (Richly & Leister, 2004; Yoshida *et al.* , 2014; Greiner and Fridman, personal communication). Therefore, we isolated the chloroplast DNA and performed nanopore sequencing.

Chloroplast DNA isolation

Ten grams fresh leaf tissue were taken and grinded in pestle mortar using liquid N₂. Grinded powder was transferred in small beaker mixed with 100 ml isolation buffer (50 mM Tris-HCl pH 8.0, 0.35 M sucrose, 7 mM EDTA, 5 mM 2-mercaptoethanol, 0.1% BSA), kept in 4°C for 5-30 min followed by filtration using 8 layer of gauge. The filtrate centrifuged at 1000Xg for 15 min and pellet dissolved in 3 ml of isolation buffer. The dissolved solution were loaded on top of 45/20% sucrose gradient (50 mM Tris-HCl pH 8.0, 0.3 sorbitol, 7 mM EDTA, sucrose 20% / 45%). Tubes centrifuge at 2000Xg for 30 min. Carefully middle layer (sucrose gradient junction) transferred to new tube and filed with 3 times volume of isolation buffer followed by centrifugation at 3000Xg for 20 min. Pellet (isolated chloroplast) was used for DNA isolation using CTAB method.

B1K accessions PCR barcoding and Nanopore Sequencing

We PCR amplified the region 19409-24572 using chloroplastic DNA of B1K accessions with LongAmp Taq-polymerase 2X mix (M0287S). Two-step PCR performed to tag with 96 different barcode carrying the universal adapter sequence (Table **S1**). After the barcoding all samples pooled together and purified by precipitation. 1µg of barcoded pooled PCR product was taken for library preparation using kit as per manufacturer protocol (SQK-LSK109 kit, Nanopore). 5-50 fmol DNA loaded in Nanopore flow cells (R9.4.1) after priming. After 24 hr run data were collected and performed the basecalling and demultiplexing with Guppy 5.0. Further barcodes aligned to reference with BWA-MEM2 using (-x ont2d) criteria and BAM files are sorted by coordinate. BAM files used as input for variant calling using Medaka version 1.4.4. VCF files from every alignment merged using a custom R script demultiplexing.

2.6 Marker designing and genotyping of F2 population

For genotyping of *DOC3.2* locus in F2 population (derived from crosses between B1K-05-07 and B1K-50-04), we identified sequence diversity using Nanopore data covering region of *DOC3.2*(Chr3H_67433882-Chr3H_67434491). We found SNP marker Chr3H_67434330 have C to T in B1K-50-04 and B1K-05-07, respectively, that resides within the *TaqI* recognition. For genotyping of F2 population, we isolated leaf DNA using with CTAB method, PCR amplified using suitable primers (Table **S1**) followed by restriction digestion using *TaqI* restriction enzyme to distinguish between three genotypes.

2.7 Arabidopsis plant material and growth condition

Arabidopsis thaliana (L.) Heynh ecotypes Col-0, homozygous mutant and over expression (OE) lines used in this study. T-DNA insertion mutant of *rpoC1* (*cs835205*) was obtained from the Arabidopsis Biological Resource Centre (ABRC, Ohio State University, Columbus, OH, USA; <https://abrc.osu.edu/>). Seed sterilization and plants growth were performed according to Tiwari *et al.* , (2021). Homozygosity of *rpoC1* mutant confirmed by polymerase chain reaction (PCR) by using gene-specific right primer with a T-DNA left border specific primer (pDAP110/ pCSA110) listed in Table **S1** . For over-expression of *RpoC1* gene from two allele (B1K-09-07 and B1K-50-04) in Col-0 background, coding sequence region (2046 bps without stop codon) were synthesized from Genewiz (www.genewiz.com) in pUC-GW-Amp vector. Further all the desired fragment were cloned in binary vector (pICH86966 Addgene) using golden gate assembly (Plant part: 1000000047 and toolkit: 1000000044, Addgene) (Figure **S3**).

RESULTS

3.1 Plasticity of life history traits in response to elevated temperature and its correspondence with plasmotype diversity

We wished to examine the effects of plasmotype diversity on barley fitness including growth and productivity while growing under ambient vs. high temperatures and to examine the possible relationship between

photosynthetic rhythm and growth plasticity. Previously, we described the generation and clock analysis of the ASHER doubled haploid population divided between carriers of the B1K-09-07 and B1K-50-04 plasmotypes. For the current study, we also developed a set of crosses between 11 wild barley accessions to achieve reciprocal hybrids lines (RHL) with few genotypes missing to achieve full half-diallel (see Methods).

In ASHER, under both HT and AT, carriers of the Hermon plasmotype flowered significantly earlier than the Ashkelon types. However, in both subpopulations, this manifested in the same thermal acceleration of flowering by more than two days (Figure 1a ; TableS2a). The reproductive traits were higher under AT vs. HT conditions (avg spike dry weight (ASDW) = 0.89 ± 0.13 vs. 0.7 ± 0.12 gr and Spikes dry weight (SpDW) = 7.8 ± 1.9 vs. 6.24 ± 1.7 gr, respectively). Plant height (PH) at harvest was also higher under AT (124.9 ± 8.5 cm) than under HT (108.1 ± 7.8 cm), although vegetative dry weight (VDW) was lower under AT, i.e., 13.1 ± 3.5 gr vs. 14.4 ± 4.7 gr in HT (FigureS4a). For SL, there was no significant difference between subpopulations (Figure 1b). However, for the SLCV, Hermon plasmotype was linked to lower stability (Fridman 2015), i.e., higher CV under HT (14.45% under HT vs. 8.8% under AT) as compared to Ashkelon (12.33% under HT vs. 9.32% under AT) (Fig. 1c). One interesting comparison is between the total vegetative and reproductive outputs. The carriers of the Ashkelon plasmotype are, on average, very plastic for the plant biomass and the derived total dry matter (Figure1d, e). In contrast, the Hermon plasmotype carriers are relatively stable for the biomass yet respond significantly to the heat with significant reduction of the SpDW (Figure 1e, f). This is in comparison to the relative stable SpDW of the Ashkelon types (Figure1f).

Unlike in the ASHER's case, in the RHL, DTF was almost identical between HT and AT (DTF = -109.9 ± 5.6 and 111.73 ± 4.97 days, respectively) (FigureS4b). Similarly, unlike the significant effects of the thermal environment on the vegetative traits, the reproductive traits were less affected; ASDW is significantly yet mildly lower under AT (0.93 ± 0.24 gr) than under HT (1.03 ± 0.27 gr). For SpDW, there was not a significant difference between environments (7.13 ± 2.2 and 7.35 ± 3.16 gr, respectively). PH was also not significantly different between environments (104.06 ± 10.17 cm in AT and 104.04 ± 12.05 cm in HT), as compared to VDW and TDM that were significantly lower under AT (11.29 ± 4 and 18.5 ± 5.5 gr) than HT (16.38 ± 6.8 and 24.13 ± 9.08 gr). SL and SLCV are significantly lower under AT condition (Figure S4b ; TableS2b). The reciprocal nature of the hybrids allowed us to group the F1 genotypes into different plasmotype subpopulations and different male parent subpopulations (representing the nucleotype). One-way ANOVA for each of these two divisions of the hybrids indicated a larger percentage variation explained (PVE) by the nucleotype (male donors) in comparison to differences between plasmotype (female donors) for a few traits (Table 1). For example, for the ASDW under HT the nucleotype factor explained 41% of trait variation (PVE=41%) vs. PVE=27% by the plasmotype. For most life history traits, however, we found higher variation explained by the plasmotype than by the nucleotype under both temperatures (AT and HT): for PH, PVE=39% vs. 30% and 33% vs. 21% under AT and HT, respectively. Higher variation explained by the plasmotype than nucleotype was true also for reproductive output, e.g., SpDW, which showed higher variance between plasmotypes under AT (PVE=35% vs. 21%) and to a lesser extent under HT (PVE=23% vs. 19% between plasmotype and nucleotype contributions).

To summarize, plants in both field experiments of the two populations accumulated more VDW on average at higher temperatures and showed lower stability between spikes, i.e., higher VDW and SLCV. The nature of the ASHER population allowed us to relate the positive correlation between increased biomass plasticity and stabilizing of the reproductive output with plasmotype diversity.

3.2 Plasmotype effects on the plasticity of life history vs circadian clock and ChlF traits in RHL

We also included a photosynthetic rhythmicity analysis to the RHL, similar to the one we previously conducted for the ASHER population, i.e., under optimal (OT) and high temperatures (HT) environments using SensyPAM platform (See Methods; (Bdolach *et al.* 2019)). We found that the amplitude was significantly higher under HT (0.03 ± 0.01) compared to OT (0.015 ± 0.006) (Figure 2a), whereas for the period, significantly higher values under OT (24.9 ± 2.6 h) compared to HT (23.3 ± 1.9 h; Fig. 2b) were observed. This clock plasticity is similar to the one described for the ASHER (Bdolach *et al.* , 2019) with acceleration of the rhythmicity under HT. Fv/Fm is significantly higher under HT (0.93 ± 0.01) in comparison to OT (0.92

± 0.01 ; Figure 2c) and significantly different for Fv/Fm_{lss} (0.9 ± 0.01 in OT vs. 0.91 ± 0.01 in HT; Fig. 2d). Mean values of NPQ_{lss} and Rfd *per se* (averaged over the time period of the measurement) were significantly different under OT in comparison to HT (NPQ_{lss} 0.66 ± 0.1 vs. 0.43 ± 0.08 and Rfd 1.6 ± 0.2 vs. 1.18 ± 0.18 ; Figure 2e, f). Overall, these results suggest that under HT, photosynthesis is more efficient than under OT.

For the clock traits in the RHL, we also found significant differences between the contributions of plasmotype and nucleotype to the variation of photosynthetic rhythm parameters (Table 1), but to a lesser extent than for fitness traits. Difference in contribution was higher when analyzing fitness traits, where the plasmotype’s PVE (34%) clearly topped the nucleotype’s PVE (22%), for period under HT. Similarly, variation in the thermal plasticity of photosynthetic rhythm’s amplitude value (measured as “delta amplitude”) between hybrids is better explained by plasmotype (32%) compared to nucleotype (24%) (Table 1).

3.3 Relationship between plasmotype and nuclear diversity and pleiotropic effects on circadian clock and life history traits

In the RHL, we wished to compare the occurrence of plasticity between the different traits. Therefore, we compared the number of reciprocal hybrids that significantly differ in the life history traits and Chl F traits (Figure 3). We clustered phenotypic traits measured in the net house as growth or reproductive and traits measured with SensyPAM as the clock or Chl F parameters. The percentage of different pairs of reciprocal hybrids was highest for Fv/Fm under OT (44.8%), and the lowest was zero hybrids for the difference of DTF under AT. If comparing the traits according to our clustering, we could see that the mean number of differing reciprocal hybrids is highest for Chl F (26.3%), second for clock traits (15%), and falling behind for growth and reproductive traits with 5.23% and 3.73%, respectively (Figure 3).

3.4 Genetic basis of temperature-dependent plasticity

Next, we used the SensyPAM platform to investigate the genetic basis for the period and amplitude of circadian photosynthetic rhythms and their thermal plasticity. To this end, we selected 285 wild barley of the B1K collection (Hubner *et al.*, 2009) from different geographic origins. We performed a GWAS analysis using the traits values *per se*; comparing genetic signals between phenotypic plasticity of the circadian parameters under OT and HT environments (see Methods; Table S3). Moreover, since the analysis of RHL (this study; Figure 2) and the ASHER populations (Bdolach *et al.*, 2019) indicated a significant effect of the plasmotype diversity on the photosynthetic rhythm plasticity, we included sequencing information from isolated chloroplast DNA for a portion of this panel (see Methods; Table S4).

We wanted to identify nuclear loci for which allelic diversity is associated with plasticity of photosynthetic rhythms. First, we increased the current coverage of Barley 1K genomic analysis by harvesting genic and intergenic DNA variation from several sources (see Supporting information and Methods). Prior to GWAS analysis, missing values were imputed with the “missForest” algorithm and filtered for markers with missing data > 0.2 , minor allele frequency < 0.03 , monomorphic and multiallelic markers. The selection process led to a final set of 13,786 informative markers for GWAS analysis (Table S5). We wished to detect QTLs with persistent effects across the two environments (OT and HT) but also with $Q \times E$ effects, i.e., loci with specific effects to a certain environment (Yamamoto & Matsunaga, 2021).

Briefly, the output of the analysis for each SNP included “Additive Main Effect” (*p.ame*), “All SNP effects” (*p.all*), “Interaction terms” (*p.int*) and a Wald score for each environment indicated the environment with the most significant effect of the locus on the trait (Table S6). By setting a threshold of $LOD > 4$, we found 102 signals for amplitude and only eight for the period. Seven of the eight signals we identified for the period are found in *p.all*, *p.int* and with the highest Wald score under HT. We could not detect signals above $LOD 4$ under OT in none of the traits. There were 17 significant signals for interactions in *P.all*, and all except one were affecting the trait under HT. There are five signals for the amplitude and seven for the period.

In a previous study, we identified several *DOCs* loci that modulated the circadian clock output in the HEB interspecific mapping population (Prusty *et al.*, 2021). Interestingly, some of these *DOC* loci are overlapping with signals in this current genome scan of the B1K, including some that contain genes reported to be involved

in the circadian clock. Of note is the gene *GIGANTEA* (*GI*) that resides in the long arm of chromosome 3. Previously, we identified a large interval on chromosome 3, *DOC3.2*, associated with significant pleiotropic effects on the clock period and growth in the field. Nevertheless, *DOC3.2*, although harboring the barley ortholog of the *GI* gene (Fowler *et al.*, 1999), stretched in the previous HEB population analysis to a distance of 45.98 Mbp (Chr3H_35066186 – Chr3H_81047480). Here, in the GWAS in the B1K collection, we identified SNPs around the *GI* gene that were significantly associated with the amplitude of the clock and its plasticity. In fact, the current SNP arrangement point to a causal variation in 150 kb downstream to the *GI* gene. Phenotypic analysis showed difference in the amplitude between two allele under HT condition while no effect was assigned to the allele in OT condition (Figure **S5**).

3.5 CNI and linkage disequilibrium (LD) between chloroplastic *RpoC1* and *DOC* loci

One primary goal of this study was to explore the plasmotype variation’s contribution to the circadian photosynthetic rhythm plasticity and growth together with the possibility of epistatic interaction with nuclear loci relevant to the clock output. Since earlier we identified variation within chloroplastic *rpoC1* as possible causal variation between B1K-09-07 and B1K-50-04 (Bdolach *et al.*, 2019), we performed a long-range Nanopore sequencing of the *RpoC1* region with chloroplast DNA isolated from 75 B1K accessions.

Table **S7** includes the identified SNP within the panel of 75 B1K accessions. In *RpoC1*, there is one distinct SNP (position *RpoC1*^{G1713T}) that divides the sequenced B1Ks into 51 accessions that carry the *RpoC1*^{1713T} allele, while the other 24 accessions carry the *RpoC1*^{1713G} allele. Notably, this SNP is a non-synonymous mutation of the *RpoC1* chloroplastic gene (changes N:AAT to K:AAG ; Table S3).

We tested the effects of two main QTL, i.e. *DOC3.2* for amplitude and *DOC5.1* for period (Figure **4a, b**), in the complete and in the smaller panels (n=285 and 75, respectively), while considering *RpoC1* variation in the later (Table **S7**). For *DOC3.2*, we noticed segregation at chr3H_67267835 between A and G only for the 51 out of 75 *RpoC1*-sequenced B1K that carry the *RpoC1*^{1713T} allele (Figure **4c**). This is compared to the other 24 carriers of the *RpoC1*^{1713G} where no segregation is found for chr3H_67267835. A strong CNI is also found between the *RpoC1* and *DOC5.1* (chr5H_648981054), a locus with significant effects on the period (Figure **4b**). While in the *RpoC1*^{1713G} background there is mild difference in the period thermal plasticity between carriers of the two *DOC5.1* allele, a more significant and even opposite directionality is found for the nuclear locus in the background of *RpoC1*^{1713T} (Figure **4b, d**).

3.6 CNI in F2 population for clock rhythmicity

To examine the QTLs found in the B1K related to circadian photosynthetic rhythms, including testing the CNI, we generated F2 population from reciprocal crosses between two wild B1K accessions, B1K-05-07 and B1K-50-04. These crosses allow the analysis of the clock output phenotype linked with segregation in the nuclear locus and comparison of this relationship in two differing chloroplast genetic backgrounds. We phenotyped and genotyped the two F2 populations (B1K-05-07 and B1K-50-04 plasmotypes; n=84 and 113, respectively) for the chr3H_67434330 near the *GI* gene (Figure **S5**). In the total F2 plants, without considering the plasmotype identity, the *DOC3.2* allele of the B1K-50-04 was associated with higher thermal plasticity for the period (accelerated clock in the transition to HT; delta=-1.34h) than the B1K-05-07 allele (delta=-0.6h) (Figure **5a**). For the amplitude, there is no difference in plasticity between B1K-05-07 and B1K-50-04 alleles (delta -0.006 and -0.008, respectively) and similar significant difference between temperatures (p=0.0003 and p=0.0006, respectively) (Figure **5b**; Table **S8**).

When we split the analysis between the two F2 populations, based on the plasmotype, we could see relatively mild differences between the two. Statistical testing using two factorial ANOVA of the interaction between the *DOC3.2* / chr3H_67434330 alleles and the plasmotypes for the period and the amplitude found significant interaction between the nucleotype and plasmotype loci only for the amplitude under OT (P=0.01) (Table **S9**). The "natural" combination of plasmotype/*GI* of B1K-05-07/05-07 has the amplitude of 0.03 and the B1K-50-04/50-04 has the amplitude of 0.032, while the "unnatural" arrangement of B1K-05-07/50-04 and B1K-50-04/05-07 has lower amplitude of 0.025. These results imply that combination of the plasmotype and *DOC3.2* / chr3H_67434330 of the same origin (either B1K-50-04 or B1K-05-07) are associated with higher

amplitude values. This could be viewed in the crisscross pattern where the mean amplitude values of two genotypic group is in opposite direction under OT (Figure 5c , right-bottom panel).

3.7 Arabidopsis complementation with barley *RpoC1* alleles confer differential clock output plasticity

Previously, the comparison between Ashkelon and Hermon’s chloroplast genomes (B1K-09-07 and B1K-50-04) identified a non-synonymous SNP at the *RpoC1* gene (position: 24530; N571K), which is part of the plastid-encoded RNA polymerase (PEP) protein complex. Based on previous reports on co-evolution between genes encoding PEP and nuclear genes (sig1-6) (Zhang *et al.*, 2015), we hypothesized that *RpoC1* could be responsible for the difference in photosynthetic rhythm parameters between the two subpopulations within ASHER (Bdolachet *et al.*, 2019). In the current study, some of the interactions we tested for the same nonsynonymous SNP in the wider B1K collection support an association to the clock plasticity and possibly to other growth traits (Figure 4). Therefore, we first tested *rpoC1* mutant in the *Arabidopsis* background. We procured T-DNA insertion *rpoC1* mutant (*cs835205*) lines that showed integration in intron region of *RpoC1* gene (Figure 6a). We analyzed the chloroplastic *rpoC1* mutant for clock phenotype and noticed that, *rpoC1* mutant showed plasticity in the period compared to wild type (WT) plants during temperature shift in short day entrainment (Table S10). Under OT, clock period in *rpoC1* mutant and WT varied between 20.71-27.44 hr and 20.8-29.08 hr, respectively, with coefficient of variance (CV) 9.28% (*rpoC1*) and 8.67% (WT). The mean period of the *rpoC1* mutant and WT plants under the two temperatures differed significantly with clock rhythm accelerated from period length of 24.28 hr under OT to 22.58 hr under HT in *rpoC1* mutant line as compared to relatively robust rhythmicity of the WT, i.e. 22.82 hr and 23.40 hr under OT and HT, respectively (Figure 6b ; S6a).

Next, we wished to compare the possible consequences of the barley *RpoC1* variation on the clock output in the heterologous *Arabidopsis* system. We therefore over-expressed (OE) the chloroplastic *RpoC1* gene alleles from B1K-09-07 and B1K-50-04 barley in Col-0 *Arabidopsis* background. To direct translocation to the chloroplast the barley we fused the chloroplastic *RpoC1* coding region with chloroplast transit peptide under the control of *CaMV35S* promoter (Figure 6c). The homozygous OE lines were analysed for clock phenotype under OT and HT condition (Table S11). The *Arabidopsis* OE lines for the B1K-09-07 *RpoC1* showed, on average, a significant plasticity or acceleration of the period during temperature shift from 23.73 to 22.18 hr, similar to the *rpoC1* mutant line (*rpoC1* : OT-23.54 hr, HT-22.41 hr). This is compared to the B1K-50-04 allele OE lines that showed robustness in the period (OT-22.93 hr, HT-22.85 hr) during temperature shift similar to WT lines (OT-23.27 hr, HT-24.23 hr) (Figure 6d ; S6b). Overall, in short day entrainment B1K-50-04 allelic OE lines and WT showed robustness while B1K-09-07 allelic OE lines and *rpoC1* mutant showed plasticity during temperature shift. Similar to mutant and WT lines, OE lines from both allele showed amplitude remain same and decelerated during temperature shift.

Discussion

4.1 Whole plant and circadian clock responses to high temperatures and their interrelationship vs pleiotropy

In this study, we found significant responses of plant growth and clock rhythmicity under elevated temperature. Comparison between early and late growth phenotypes showed that plants growing in high temperatures initially gain some growth advantage, as reflected by the higher tiller heights measured at about one month after transplanting. However, at the final time of harvest the heat correlated significantly with reduced height, biomass and reproductive output (Figure S4). In addition, we found that heat is related with loss of robustness of the growth as could be viewed in the significant elevated CV of the spikes. Interestingly, the population of inbreds (ASHER DH) seemed to be more affected than the RHL, with the latter maintaining, for example, a similar mean for PH and SL values. These differences in the stability of hybrids was reported in many plant species and might be related with higher allelic heterogeneity across the genome (Fridman 2015), which to some extent may allow the plant to show a wider reaction norm as suggested in biochemical models of heterosis (Goff, 2011).

The experiments we describe in this study were all making use of wild barley plants and their derivatives. Although wild and cultivated barley belong to the same primary gene pool and easily crossed to obtain fertile

interspecific populations (Wendler, 2018), the comparison between the results of current study to the one conducted with interspecific HEB population raise at least one interesting difference in the adaptive behavior of the plants. In the previous study (Prusty *et al.*, 2021), we identified a significant pleiotropy of the *DOC3.2*, a locus that affected thermal plasticity of the vegetative growth and the clock amplitude. Carriers of the wild alleles showed increasing amplitude under higher temperature, and at the same time increased biomass but with lesser grain yield. Here, while analyzing the relationship between plasmotype diversity to clock and fitness traits plasticity we identified a different trend. There was an opposite relationship between plasticity of growth and reproductive output; under higher temperature increased biomass (and more pronounced plasticity of the clock) was correlated with stability of the reproductive output (Figure 1). The carrier of the B1K-50-04 plasmotype that kept stable growth under higher-temperature had a significant loss of average spike weight. These differences indicate that while wild alleles have the potential to benefit crop plants as often proposed (Dakhiya & Green, 2023), the interactions of the nuclear and plasmotype diversity should be tested in the relevant genetic and management “environments”. This approach is now followed in a new interspecific cytonuclear multi-parent population (CMPP) that we are currently testing for clock and for agricultural performance (manuscript in preparation).

4.2 Non-random association and interactions between DOC loci and chloroplastic RpoC1

Since its establishment, the Barley1K infrastructure has been an instrumental research tool to explore landscape genomics (Hubner *et al.*, 2009; Hübner *et al.*, 2013; Chang *et al.*, 2022), plant biotic and abiotic interactions (Sade *et al.*, 2012; Dakhiya *et al.* 2017; Alegria Terrazas *et al.* 2020; Dakhiya & Green 2023), and more recently as reference for the whole barley Pan genome (Jayakodi *et al.* 2020). Here, we extend the use of the B1K by 1) developing a more dedicated genotyping platform for the wild barley to allow GWAS and 2) start exploring the chloroplast variation and its possible relationship with fitness traits. At first glance, the results obtained in this study could not directly be translated to crop improvement, mainly since, as we show here, adaptation strategies in the wild and agricultural set up are different (biomass vs reproductive output responses to heat, see above). However, the B1K resource bear genetic attributes that could assist in targeting specific genes and gene complexes mainly owing to the non-randomness and long years of recombination within and between nuclear and chloroplastic genomes and the way natural selection works on these intra and inter-loci combinations. For the nuclear genome, it is clear that the LD decay is enormously shorter than that one could find in interspecific populations (Morrell *et al.* 2005). *DOC3.2* may be a good example for this “gene discovery” use of the B1K panel for zooming-in on a causal diversity that otherwise would be delimited to 7.7 Mbp in using the interspecific population (Prusty *et al.*, 2021). Here, a closer look on at the allelic diversity indicates the QTL for amplitude under HT in long days, which was identified in the previous study, most probably corresponds to the signal identified at chr3H_67267835. This marker is flanked by the non-significant markers chr3H_66,838,086 and chr3H_68,838,244, therefore limiting the source of phenotypic variation to approximately 2 Mbp for this QTL.

For the chloroplast genome per se, and for the allelic combinations with the nuclear genome, this study shows clearly the rich diversity repertoire found in this organelle within the wild (Table S7) and its relevance to plant adaptation. Moreover, we could identify both LD and CNI between DOC and the *rpoC1* alleles in the B1K panel, where in an extreme case of the *DOC3.2* this locus showed segregation only among carriers of the *RpoC1^{G1713T}*. Non-random association of alleles in the nucleus and cytoplasmic organelles, or cyto-nuclear LD, is both an important component of a number of evolutionary processes and a statistical indicator of others (Fieldset *et al.*, 2014). We also followed up on the GWAS to examine inheritance of these CNI interaction, and, beyond validating the environment-specific effects of the *DOCs*, we could also get indication for preferred homogeneity of the CNI. For example, in the case of CNI for the *DOC5.1* combination of plasmotype and nuclear alleles from same origin (B1K-05-07 or B1K-50-07, the two parental lines of the F2) was associated with higher amplitude. This correspond well with recent study which suggested that increased amplitude under heat is positively correlated with higher plant vitality (Dakhiya & Green, 2023). In case of cereal evolution, it was hypothesized and in silico tested that in ancient hybridization, such as the one between the A and D-genomes of modern wheat there has been biased maintenance of maternal A-genome ancestry in nuclear genes encoding cytonuclear enzyme complexes (CECs) (Li *et al.*, 2019). It is tempting to hypothesize

that we observe such scenario in the case of the DOC and *rpoC1* loci in the B1K.

4.3 Validation of the *poC1*^{G1713T} causality in Arabidopsis and implication for understanding PEP complex role in clock plasticity

Our heterologous expression of the B1K-50-04 and B1K-09-07 *RpoC1* alleles in the *Arabidopsis* chloroplast support the role of N571K substitution in manifesting heat responses and changes in the photosynthetic rhythmicity (Figure 6). Zooming in on this significant and hitherto unknown relationship between PEP variation and clock thermal plasticity will require a more thorough analysis of more advanced and isogenic lines. In the PEP complex, one major functional group is comprised of PAPs involved in DNA/RNA metabolism and gene expression regulation, while the second group is related to redox regulation and reactive oxygen species protection (Steiner *et al.* 2011). Moreover, the PEP is somehow coordinated with the nuclear encoding RNA polymerase (Pfannschmidt *et al.*, 2015). Therefore, presumably non-synonymous variations (such as those between *RpoC2* alleles that we identified but not yet tested; Table S7) could be as effective as non-synonymous ones (between *RpoC1* alleles) in the functionality and variation we observed. It would be therefore required to look at different layers (transcriptome, proteome) between nearly isogenic and not necessarily knockout mutant lines to achieve relevant causal variation. Recent developments in plastid gene editing, also in cereals, may assist in generating and analyzing both types of mutations in barley and learn how they might modulate physiology and development of the plant under normal and high temperatures. Recent experiments suggest that most recent developments of TALEN-based allele editing tested in *Arabidopsis* (Nakazato *et al.*, 2021) could also be applied in barley (Fridman and Arimura, Personal communication) to allow such multi-layer analysis of isogenic mutants.

Conclusions

This study indicates that the relationship between plasticity of the clock under warming with robustness of plants could have a significant effect on shaping the cytonuclear diversity. However, one way of testing the possible cause behind these LD and CNI will require cloning of the underlying genes in the DOC and figuring out how they may interact with chloroplastic genes such as *rpoC1*, and to learn what makes one allele different than other and what cellular mechanisms may be involved.

ACKNOWLEDGEMENTS

We thank Dr Stephan Greiner (Max-Planck-Institut für Molekulare Pflanzenphysiologie, Golm, Germany) for sharing barley chloroplasts sequence data. The authors are grateful to Royi Levav Oded Anner and Daniel Shamir (SensyTIV, Amiel, Israel) for their assistance in maintaining the SensyPAM as a system for measuring circadian rhythms. We also wish to thank the technical assistance of laboratory member Avital Beery and Orit Amir-Segev.

LIST OF AUTHOR CONTRIBUTIONS

E.B., L.D.T. and E.F. designed the experiments, collected, analyzed and interpreted data, with A.B., and wrote the manuscript. M.R.P. and A.F.D. collected and designed the B1K SNP platform, and E.Y. performed the QxE GWAS. E.B., L.D.T., M.R.P., S.B., E.Y., were involved in the data analyses, their interpretation and in writing the manuscript.

References:

- Alegria Terrazas R., Balbirnie-Cumming K., Morris J., Hedley P.E., Russell J., Paterson E., . . . Bulgarelli D. (2020) A footprint of plant eco-geographic adaptation on the composition of the barley rhizosphere bacterial microbiota. *Scientific Reports* **10**, 12916.
- Bdolach E., Prusty M.R., Faigenboim-Doron A., Filichkin T., Helgerson L., Schmid K.J., . . . Fridman E. (2019) Thermal plasticity of the circadian clock is under nuclear and cytoplasmic control in wild barley. *Plant Cell and Environment* **42**: 3105-3120.
- Belbin F.E., Noordally Z.B., Wetherill S.J., Atkins K.A., Franklin K.A. & Dodd A.N. (2017) Integration

of light and circadian signals that regulate chloroplast transcription by a nuclear-encoded sigma factor. *New Phytologist* **213** .

Bineau E., Diouf I., Carretero Y., Duboscq R., Bitton F., Djari A., ... Causse M. (2021) Genetic diversity of tomato response to heat stress at the QTL and transcriptome levels. *The Plant Journal* **107** : 1213-1227.

Chang C.W., Fridman E., Mascher M., Himmelbach A. & Schmid K. (2022) Physical geography, isolation by distance and environmental variables shape genomic variation of wild barley (*Hordeum vulgare* L. ssp. *spontaneum*) in the Southern Levant. *Heredity* **128**: 107–119

Dakhiya Y. & Green R. (2023) The importance of the circadian system for adaptation to heat wave stress in wild barley (*Hordeum spontaneum*). *Environmental and Experimental Botany* **206** , 105152.

Dakhiya Y., Hussien D., Fridman E., Kiflawi M. & Green R. (2017) Correlations between circadian rhythms and growth in challenging environments. *Plant Physiology* **173** , 1724–1734.

Ekiz H., Kiral A.S., Akçin A. & Simsek L. (1998) Cytoplasmic effects on quality traits of bread wheat (*Triticum aestivum* L.). *Euphytica* **100** , 189–196.

Fields P.D., McCauley D.E., McAssey E.V. & Taylor D.R. (2014) Patterns of cyto-nuclear linkage disequilibrium in *Silene latifolia*: genomic heterogeneity and temporal stability. *Heredity* **112** , 99–104.

Flood P.J., Theeuwen T.P.J.M., Schneeberger K., Keizer P., Kruijer W., Severing E., ... Wijnker E. (2020) Reciprocal cybrids reveal how organellar genomes affect plant phenotypes. *Nature Plants* **6** , 13–21.

Fowler S., Lee K., Onouchi H., Samach A., Richardson K., Morris B., ... Putterill J. (1999) GIGANTEA: A circadian clock-controlled gene that regulates photoperiodic flowering in *Arabidopsis* and encodes a protein with several possible membrane-spanning domains. *EMBO Journal* **18** , 4679–4688.

Frei U., Peiretti E.G. & Wenzel G. (2003) Significance of cytoplasmic DNA in plant breeding. In *Plant Breeding Reviews* . (ed J. Janick), pp. 175–210.

Frei U., Peiretti E.G. & Wenzel G. (2010) *Significance of Cytoplasmic DNA in Plant Breeding* **23** .

Fridman E. (2015) Consequences of hybridization and heterozygosity on plant vigor and phenotypic stability. *Plant Science* **232** , 35–40.

Goff S. a (2011) A unifying theory for general multigenic heterosis: energy efficiency, protein metabolism, and implications for molecular breeding. *The New phytologist* **189** , 923–37.

Gordon V.S. & Staub J.E. (2011) Comparative analysis of chilling response in cucumber through plastidic and nuclear genetic effects component analysis. *Journal of the American Society for Horticultural Science* **136** , 256–264.

Gould P.D., Diaz P., Hogben C., Kusakina J., Salem R., Hartwell J. & Hall A. (2009) Delayed fluorescence as a universal tool for the measurement of circadian rhythms in higher plants. *Plant Journal* **58** , 893–901.

Groen S.C., Joly-Lopez Z., Platts A.E., Natividad M., Fresquez Z., Mauck W.M., ... Henry A. (2022) Evolutionary systems biology reveals patterns of rice adaptation to drought-prone agro-ecosystems. *The Plant Cell* **34** , 759–783.

Hübner S., Bdolach E., Ein-Gedy S., Schmid K.J., a. K. & Fridman E. (2013) Phenotypic landscapes: Phenological patterns in wild and cultivated barley. *J Evol Biol* **26** , 163–174.

Hubner S., Höffken M., Oren E., Haseneyer G., Stein N., Graner A., ... Fridman E. (2009) Strong correlation of wild barley (*Hordeum spontaneum*) population structure with temperature and precipitation variation. *Molecular Ecology* **18** , 1523–1536.

Jayakodi M., Padmarasu S., Haberer G., Bonthala V.S., Gundlach H., Monat C., ... Stein N. (2020) The barley pan-genome reveals the hidden legacy of mutation breeding. *Nature* **588** : 284–289.

- Joseph B., Corwin J.A., Li B., Atwell S. & Kliebenstein D.J. (2013) Cytoplasmic genetic variation and extensive cytonuclear interactions influence natural variation in the metabolome. *eLife* **2** , e00776.
- Kromdijk J., Głowacka K., Leonelli L., Gabilly S.T., Iwai M., Niyogi K.K. & Long S.P. (2016) Improving photosynthesis and crop productivity by accelerating recovery from photoprotection. *Science* **354** .
- Li C., Sun X., Conover J.L., Zhang Z., Wang J., Wang X., ... Gong L. (2019) Cytonuclear Coevolution following Homoploid Hybrid Speciation in *Aegilops tauschii* . *Molecular Biology and Evolution* **36** , 341–349.
- Looseley M.E., Bayer M., Bull H., Ramsay L., Thomas W., Booth A., ... Russell J. (2017) Association mapping of diastatic power in uk winter and spring barley by exome sequencing of phenotypically contrasting variety sets. *Frontiers in Plant Science* **8** , 1–13.
- Maurer A., Draba V., Jiang Y., Schnaithmann F., Sharma R., Schumann E., ... Pillen K. (2015) Modelling the genetic architecture of flowering time control in barley through nested association mapping. *BMC Genomics* **16** , 1–12.
- Merchuk-Ovnat L., Silberman R., Laiba E., Maurer A., Pillen K., Faigenboim A. & Fridman E. (2018) Genome scan identifies flowering-independent effects of barley HsDry2.2 locus on yield traits under water deficit. *Journal of Experimental Botany* **69** , 1765–1779.
- Morrell P.L., Toleno D.M., Lundy K.E. & Clegg M.T. (2005) Low levels of linkage disequilibrium in wild barley (*Hordeum vulgare* ssp. *spontaneum*) despite high rates of self-fertilization. *Proceedings of the National Academy of Sciences of the United States of America* **102** , 2442–7.
- Nakazato I., Okuno M., Yamamoto H., Tamura Y., Itoh T., Shikanai T., ... Arimura S. ichi (2021) Targeted base editing in the plastid genome of *Arabidopsis thaliana*. *Nature Plants* **7** .
- Pfannschmidt T., Blanvillain R., Merendino L., Courtois F., Chevalier F., Liebers M., ... Lerbs-Mache S. (2015) Plastid RNA polymerases: Orchestration of enzymes with different evolutionary origins controls chloroplast biogenesis during the plant life cycle. *Journal of Experimental Botany* **66** .
- Prusty M.R., Bdolach E., Yamamoto E., Tiwari L.D., Silberman R., Doron-Faigenbaum A., ... Fridman E. (2021) Genetic loci mediating circadian clock output plasticity and crop productivity under barley domestication. *New Phytologist* **230** : 1787-1801.
- Ravi M., Marimuthu M.P.A., Tan E.H., Maheshwari S., Henry I.M., Marin-Rodriguez B., ... Zhu F. (2014) A haploid genetics toolbox for *Arabidopsis thaliana*. *Nature Communications* **5** : 5334
- Rees H., Duncan S., Gould P., Wells R., Greenwood M., Brabbs T. & Hall A. (2019) A high-throughput delayed fluorescence method reveals underlying differences in the control of circadian rhythms in *Triticum aestivum* and *Brassica napus*. *Plant Methods* **15** .
- Richly E. & Leister D. (2004) NUPTs in sequenced eukaryotes and their genomic organization in relation to NUMTs. *Molecular Biology and Evolution* **21** .
- Roux F., Mary-Huard T., Barillot E., Wenes E., Botran L., Durand S., ... Budar F. (2016) Cytonuclear interactions affect adaptive traits of the annual plant *Arabidopsis thaliana* in the field. *Proceedings of the National Academy of Sciences* **113** , 3687–3692.
- Sade N., Gebremedhin A. & Moshelion M. (2012) Risk-taking plants: anisohydric behavior as a stress-resistance trait. *Plant Signal Behav* **7** , 767–70.
- Sanetomo R. & Gebhardt C. (2015) Cytoplasmic genome types of European potatoes and their effects on complex agronomic traits. *BMC Plant Biology* **15** , 162.
- Schmalenbach I., March T.J., Pillen K., Bringezu T. & Waugh R. (2011) High-resolution genotyping of wild barley introgression lines and fine-mapping of the threshability locus *thresh-1* using the illumina goldengate assay. *G3: Genes, Genomes, Genetics* **1** , 187–196.

Steiner S., Schröter Y., Pfalz J. & Pfannschmidt T. (2011) Identification of essential subunits in the plastid-encoded RNA polymerase complex reveals building Blocks for Proper plastid development. *Plant Physiology* **157** .

Tang Z., Hu W., Huang J., Lu X., Yang Z., Lei S., ... Xu C. (2014) Potential involvement of maternal cytoplasm in the regulation of flowering time via interaction with nuclear genes in maize. *Crop Science* **54** .

Tindall A.J., Waller J., Greenwood M., Gould P.D., Hartwell J. & Hall A. (2015) A comparison of high-throughput techniques for assaying circadian rhythms in plants. *Plant Methods* **11** , 32.

Tiwari L.D., Kumar R., Sharma V., Sahu A.K., Sahu B., Naithani S.C. & Grover A. (2021) Stress and development phenotyping of Hsp101 and diverse other Hsp mutants of *Arabidopsis thaliana*. *Journal of Plant Biochemistry and Biotechnology* **30** , 889–905.

Wendler N. (2018) The Genomes of the Secondary and Tertiary Gene Pools of Barley. In *The Barley Genome* . Compendium of Plant Genomes, (eds N. Stein & G.J. Muehlbauer), pp. 337–344. Springer International Publishing, Cham: Springer International Publishing, 337–344.

Yamamoto E. & Matsunaga H. (2021) Exploring efficient linear mixed models to detect quantitative trait locus-by-environment interactions. *G3 Genes|Genomes|Genetics* **11** , jkab119.

Yoshida T., Furihata H.Y. & Kawabe A. (2014) Patterns of genomic integration of nuclear chloroplast DNA fragments in plant species. *DNA Res* .

Zhang J., Ruhlman T.A., Sabir J., Blazier J.C. & Jansen R.K. (2015) Coordinated Rates of Evolution between Interacting Plastid and Nuclear Genes in Geraniaceae. *The Plant Cell* **27** , 563–573.

Legends

Table 1. Contribution of the nucleotype and plasmotype diversity to phenotypic differences between reciprocal hybrids. Tiller height at two time points and the rate between them, Days to flowering (DTF), Average Spike dry weight (ASDW), Plant height (PH), Spike length (SL), spike length CV, Spikes dry weight (SpDW), Total dry matter (TDM) and Vegetative dry weight (VDW) in the nethouse under ambient temperature (AT) and high temperature (HT). For clock and Chl F traits: Amplitude, Period, delta Amplitude (dAMP), delta Period (dPeriod), Fv/Fm, F/Fmlss, NPQlss and Rfd in SensyPAN under optimal temperature of 22°C (OT) or high temperature of 32°C (HT) and the delta HT-OT.

Figure 1. Thermal plasticity of life history traits is under cytoplasmic control in wild barley. Reaction norms of life history traits in the ASHER population depicting the average responses to mild heat of lines carrying either of the two parental plasmotypes. Differential response between the carriers of Ashkelon (dotted line) and Hermon (solid line) plasmotype for (a) Spikes dry weight (SpDW), (b) Spike length (SL), (c) Spike length CV (SLCV), (d) Vegetative dry weight (VDW), (e) Total dry matter (TDM) and (f) Spikes dry weight (SpDW). Levels not connected by same letter are significantly different in student's t-test ($P < 0.05$). Different letters indicate the one way ANOVA test for significant differences.

Figure 2. Chlorophyll florescence and circadian clock rhythmicity in barley reciprocal hybrids lines grown under OT and HT . Distribution and box plot of clock output rhythmicity: (a) Amplitude, and (b) Period, and for mean chlorophyll florescence traits: (c) Fv/Fm, (d) Fv/Fmlss, (e) NPQlss and (f) Rfd under optimal temperature (OT, black) and high temperature (HT, gray) in the reciprocal hybrids lines population. For each student's t-test, the p value is depicted as *: $P < 0.05$, **: $P < 0.01$ or ***: $P < 0.001$.

Figure 3. Proportion of crosses with significant difference between reciprocal hybrids for phenotypic traits, under OT or AT and HT. Life history traits include: Tiller height (TH) and tiller number (TN) at two time points and the rate between them, Days to flowering (DTF), Average Spike dry weight (ASDW), Plant height (PH), Spike length (SL), spike length CV (SLCV), Spikes dry weight (SpDW), Total dry matter (TDM) and Vegetative dry weight (VDW) for plants in the nethouse under ambient temperature (AT) and high temperature (HT). For clock and Chl F traits: Amplitude, Period, delta

Amplitude (dAMP), delta Period (dPeriod), Fv/Fm, F/Fm_{lss}, NPQ_{lss} and Rfd in SensyPAM under optimal temperature of 22°C (OT) or high temperature of 32°C (HT) and the delta HT-OT. The mean for each type of traits is depicted: Growth or reproductive traits in the greenhouse experiment, and clock or Chl F in the SensyPAM.

Figure 4. Cytonuclear interaction (CNI) in the B1K collection between the chloroplastic *rpoC1* gene and DOCs loci under OT and HT conditions Effects for (a) Amplitude for DOC3.2, and for (b) Period for DOC5.1 (c) CNI between DOC3.2 (chr3H_67267835) and *rpoC1*¹⁷¹³ allele for amplitude. (d) CNI between DOC5.1 (chr5H_648981054) and *rpoC1*¹⁷¹³ allele for period per se (left) and for its plasticity (right). Different letters indicate the one-way ANOVA test for significant differences.

Figure 5. B1K F2 population showing clock phenotype and effect of plasmotype in reciprocal lines. (a) Period, and (b) Amplitude, for mean chlorophyll fluorescence traits in B1K-05-07 and B1K-50-04 F2 population under OT (solid line) and HT (dotted line) conditions for GI gene. Role of plasmotype in clock, (c) Period, and (d) Amplitude, between B1K-05-07 (dotted line) and B1K-50-04 (solid line) in F2 population under OT and HT conditions. Different letters indicates the one-way ANOVA test for significant differences.

Figure 6. Differential clock plasticity in Arabidopsis is linked with disruption of *rpoC1* and with overexpression barley alleles. (a) Schematic diagram showing T-DNA insertion in *RpoC1* gene (AtCG00180). Box showing the exon and line showing intron region. (b) Period phenotype of *rpoC1* and WT plants in OT and HT conditions. (c) Schematic diagram showing T-DNA of CaMV35S-Ch transit-RpoC1 construct of B1K-09-07 and B1K-50-04 alleles. (d) Period phenotype of *rpoC1*, OE-RpoC1 alleles and WT plants under OT and HT conditions. Different letters indicate the one-way ANOVA test for significant differences.

Supporting information

Table S1. List of primers used in this study.

Table S2a. The field phenotype of the ASHER population.

Table S2b. The field and SensyPAM phenotype of the reciprocal hybrids.

Table S3. SensyPAM phenotype of the B1K.

Table S4. The SNP diversity in 18Kb chloroplast region as determined by long-range Nanopore sequencing for selected B1K lines.

Table S5. Total 13,786 SNP informative SNP markers for GWAS analysis.

Table S6. The GWAS results for clock traits in B1K panel.

Table S7. The SNP variation of chloroplastic *rpoC1* and *rpoC2* region among 75 B1K accessions.

Table S8. The Sensypam clock phenotype and genotype at the chr3H_67267835 (150Kb from GIGANTEA) in two reciprocal segregating F2 populations

Table S9. ANOVA test for cytonuclear interactions underlying clock trait variation between chr3H_67267835 and plasmotype in reciprocal F2 populations.

Table S10. SensyPAM phenotype of the *rpoC1* mutant and WT plants.

Table S11. SensyPAM phenotype of the *rpoC1* mutant, OE-*rpoC1*-09, OE-*rpoC1*-50 and WT plants.

Figure S1. Daily temperature during the high and ambient temperature treatments (HT and AT, respectively) field experiments. We achieved high temperature treatment (HT) by covering half of the insect-proof with nylons and heating with electric heaters (3KW; Galon fans and pumps Ltd, Nehora, Israel). The second half of the nethouse remained with only net walls and ventilated with a large fan to take out the hot air for the ambient temperature treatment (AT).

Figure S2. Schematic diagram showing the workflow utilized for selecting informative SNPs for the GWAS analysis.

Figure S3. Schematic diagram showing the OE-RpoC1 cloning strategy. Different fragment were taken from diverse vector construct using *BsaI* restriction enzymes in binary vector pICH86966 by golden gate assembly.

Figure S4. Mild increase in temperature has significant effect on plant performance in the field. Distribution and box plot of life history traits under ambient temperature (AT, black) and high temperature (HT, gray) **(a)** ASHER DH population and **(b)** reciprocal hybrids lines. Life history traits include Tiller height at two time points and the rate between them, Average Spike dry weight, Days to flowering (DTF), Spike length (SL), Spikes dry weight (SpDW), Plant height (PH), Vegetative dry weight (VDW) and Total dry matter (TDM). For each student's t-test between HT and AT, the p value is depicted as *: $P < 0.05$, **: $P < 0.01$ or ***: $P < 0.001$.

Figure S5. (a) Physical map of DOC3.2 loci and their coordinates. Significant marker and GI gene were shown in their respective positions. **(b)** Significant marker (Chr3H_67267835) in DOC3.2 loci showing the amplitude phenotype in short day (SD) and long day (LD) in changing environment.

Figure S6. Statistics analysis of *rpoC1* , OE lines and WT plants. **(a)** Each pair student's t-test **(b)** one way ANOVA test.

Hosted file

Table 1.docx available at <https://authorea.com/users/561760/articles/609066-cytonuclear-diversity-underlying-clock-and-growth-adaptation-to-warming-environments-in-wild-barley-hordeum-vulgare-ssp-spontaneum>

Hosted file

CNI B1K plasticity Figures 301122.pptx available at <https://authorea.com/users/561760/articles/609066-cytonuclear-diversity-underlying-clock-and-growth-adaptation-to-warming-environments-in-wild-barley-hordeum-vulgare-ssp-spontaneum>

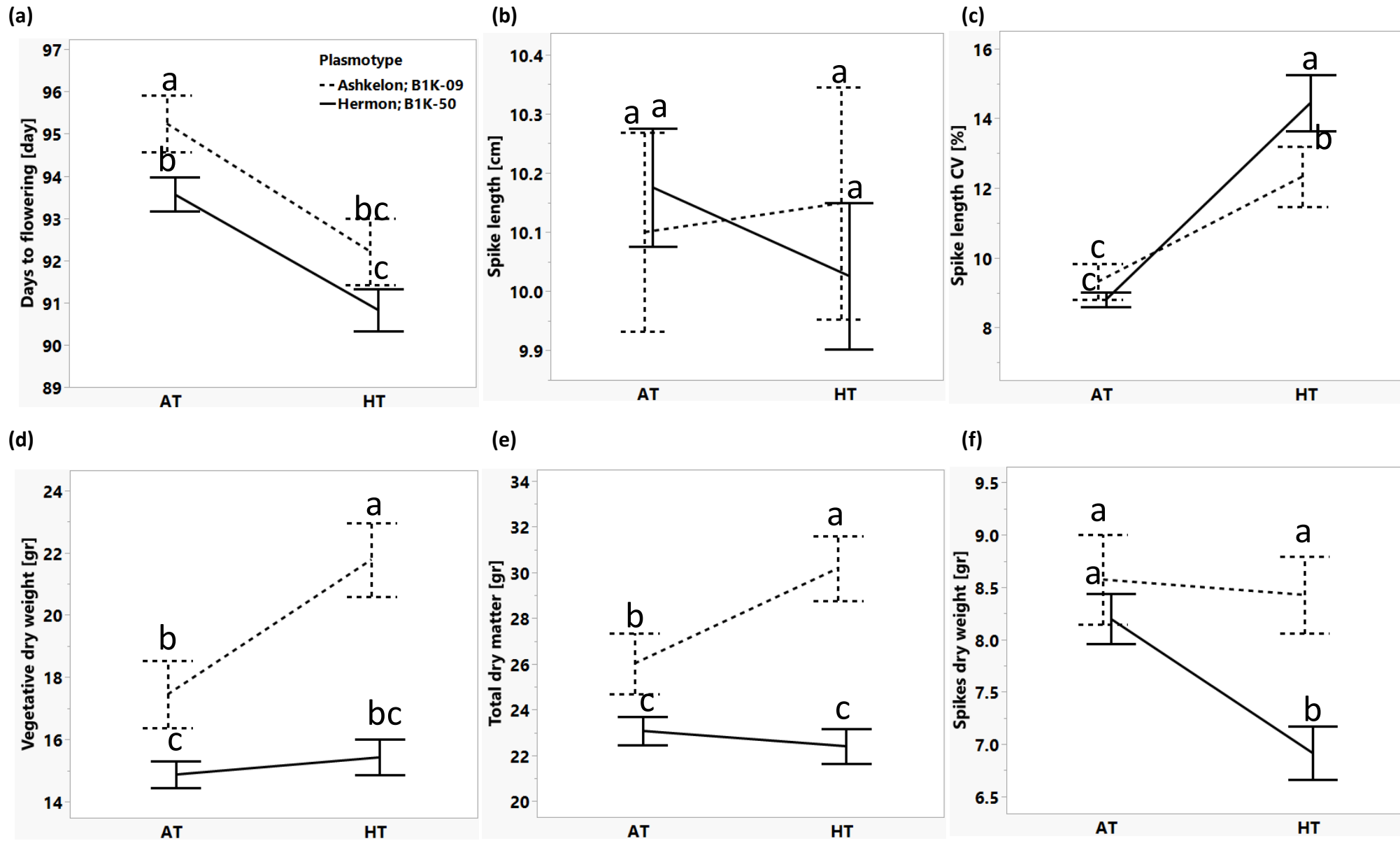


Fig. 1.

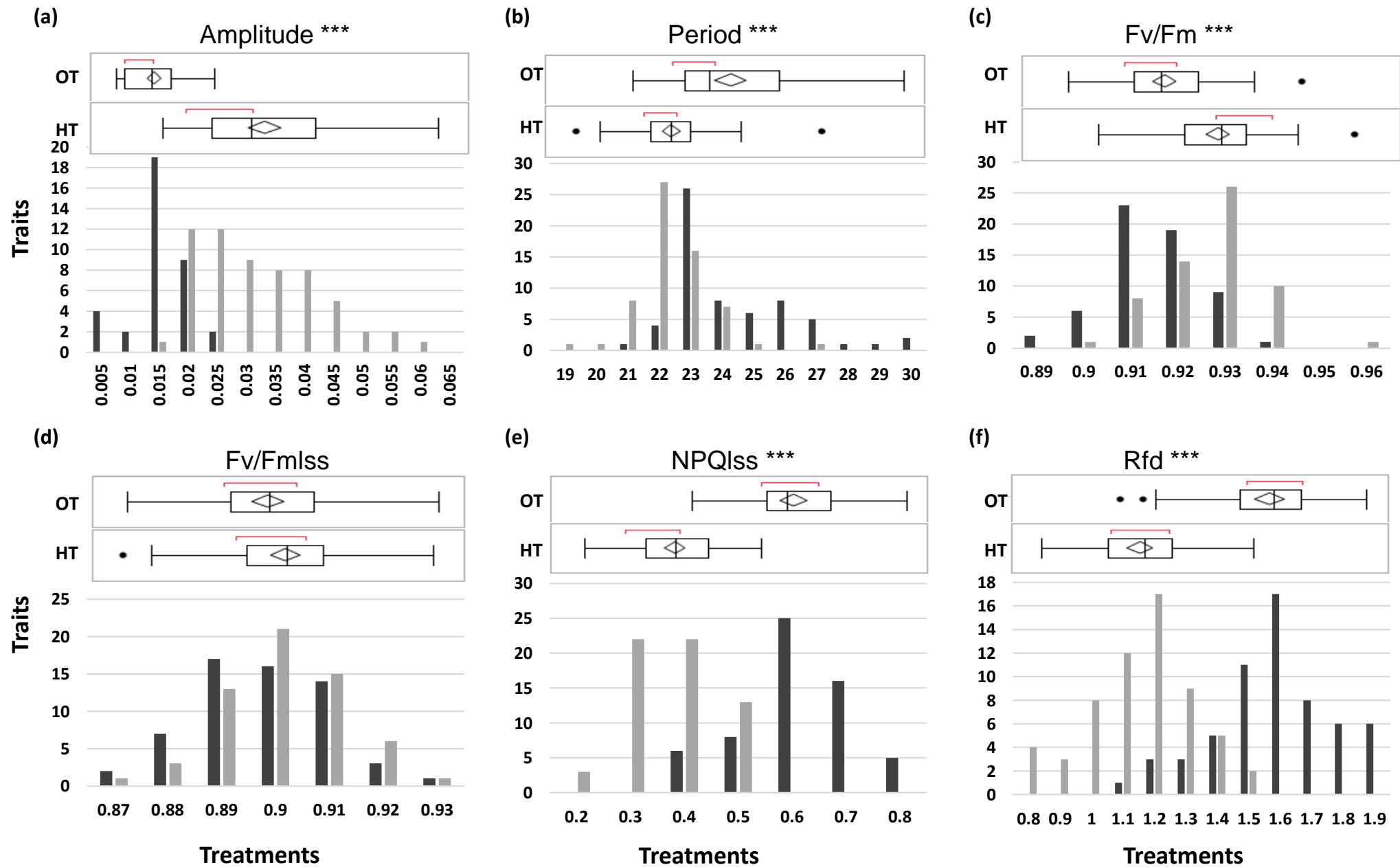


Fig. 2.

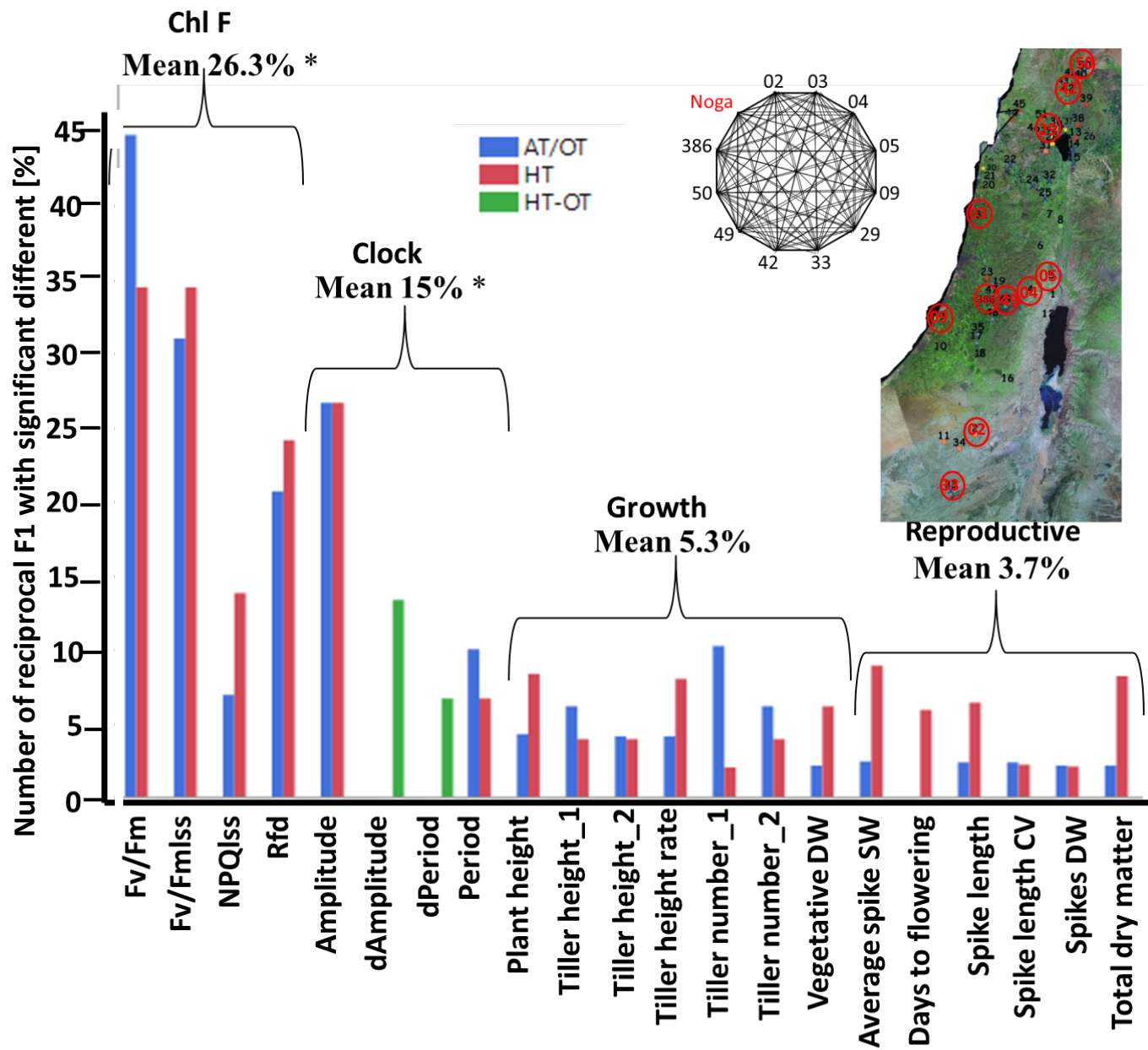


Fig. 3.

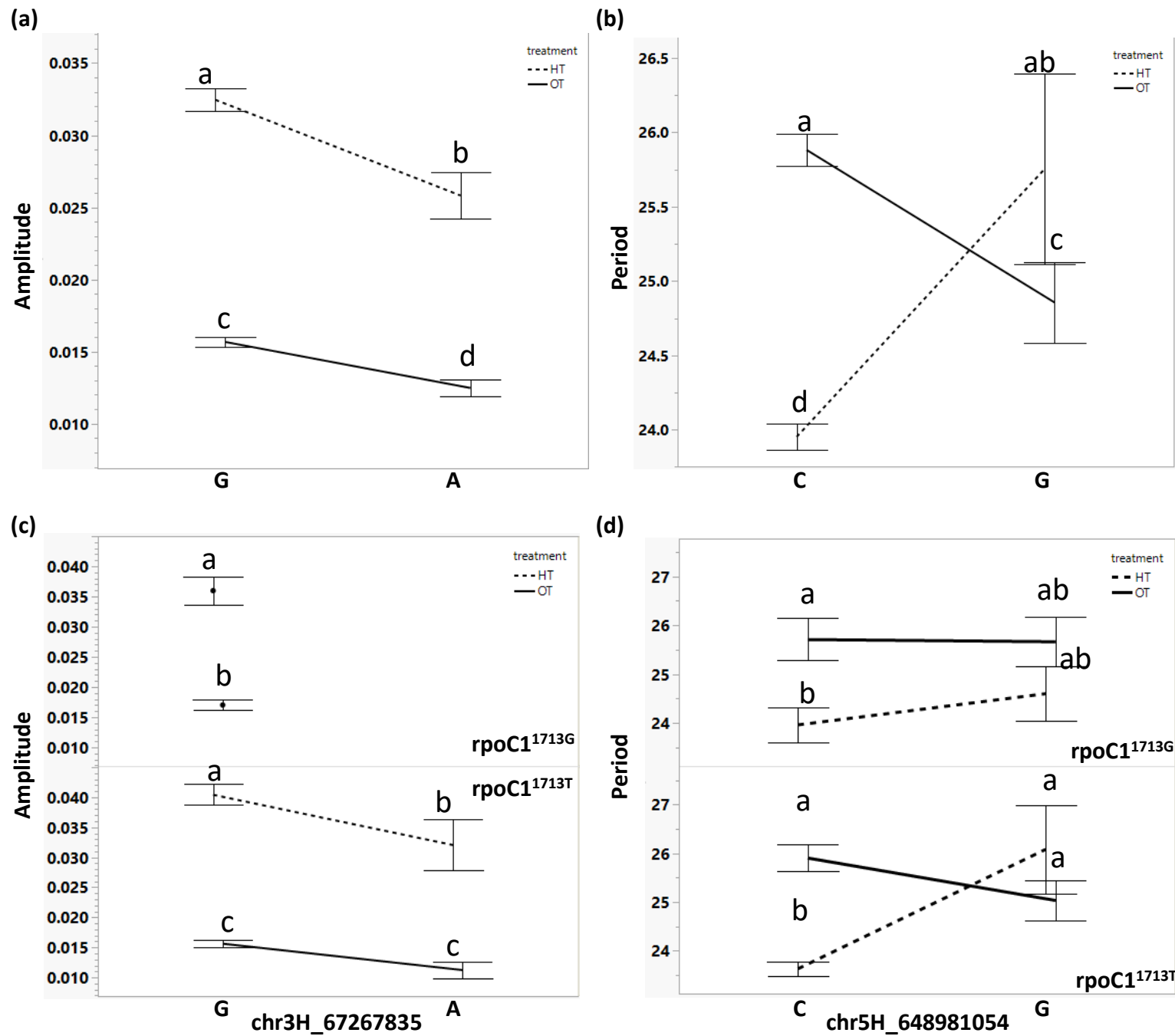


Fig. 4.

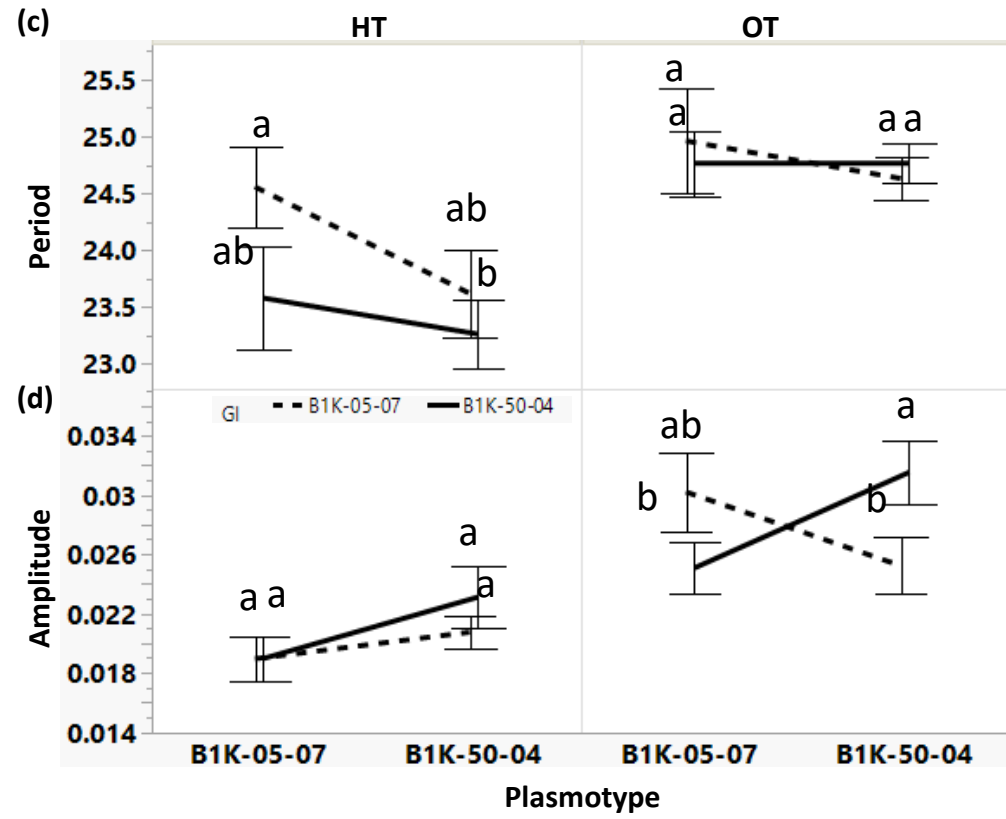
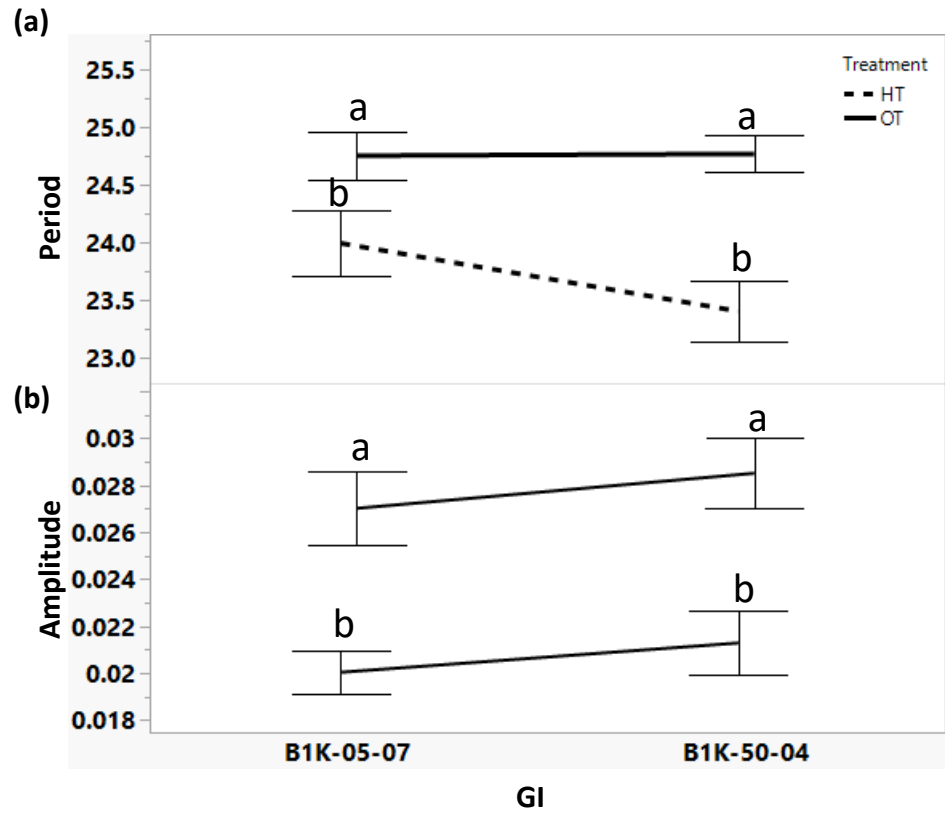


Fig. 5.

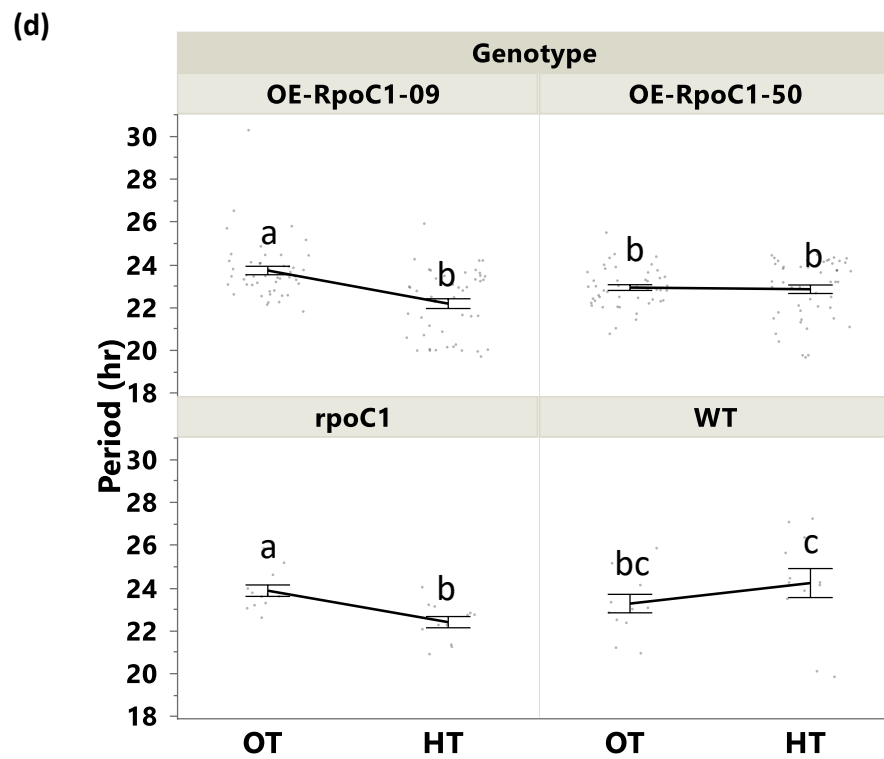
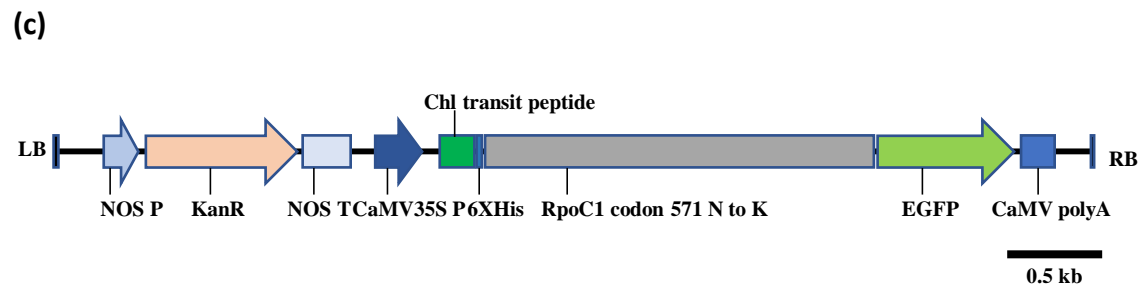
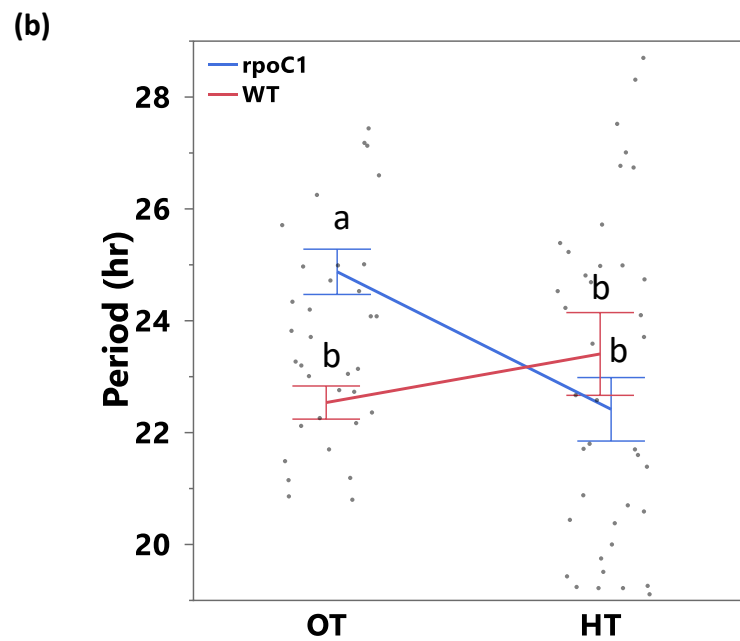
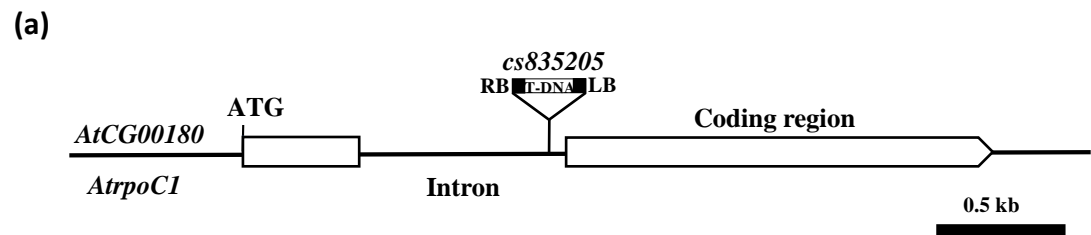


Fig. 6.